H. Santo[1]

Centre for Offshore Research & Engineering,
Department of Civil
and Environmental Engineering,
National University of Singapore,
1 Engineering Drive 2,
Singapore 117576
e-mail: ceehs@nus.edu.sg

P. H. Taylor

R. Eatock Taylor

Centre for Offshore Research & Engineering,
Department of Civil
and Environmental Engineering,
National University of Singapore,
1 Engineering Drive 2,
Singapore 117576;
Department of Engineering Science,
University of Oxford,
Oxford OX1 3PJ, UK

Y. S. Choo

Centre for Offshore Research & Engineering,
Department of Civil
and Environmental Engineering,
National University of Singapore,
1 Engineering Drive 2,
Singapore 117576

Average Properties of the Largest Waves in Hurricane Camille

*Ocean waves are known to be both random in time and nonlinear. Surface elevation time histories measured in the Gulf of Mexico during Hurricane Camille in 1969 are re-analyzed. The average shapes of large crests and deep troughs in time are shown to be close to symmetric around the instant when the maximum (or minimum) occurs, with only slight evidence of asymmetry from wave breaking in the time histories. There is considerable vertical asymmetry with higher and sharper crests and smaller and more rounded troughs. Overall, the analysis supports the use of a focused wave group based on the scaled autocorrelation function (NewWave) as proposed by Lindgren and Boccotti, with sum harmonic corrections. There is a very small second order difference setup for both large crests and troughs, consistent with considerable directional spreading in the hurricane sea-state. This spreading is likely to be larger than that usually assumed for non-tropical winter storms. The spectral tail is shown to have a decay rate proportional to –4.5 power law midway between the classical JONSWAP (Phillips) –5 form and the –4 slope proposed by Battjes et al. (1987, "A Reanalysis of the Spectra Observed in JONSWAP," J. Phys. Oceanogr., **17**(8), pp. 1288–1295) as a correction to JONSWAP.* [DOI: 10.1115/1.4006930]

1 Introduction

Wave-in-deck loading has always been a major consideration in the design of offshore platforms. The threshold for this to occur is the tallest wave crest in a storm being as high as the air-gap for the structure. Thus, a thorough understanding of the behavior of extreme waves is particularly important.

Hurricane Camille was a Category V hurricane, the most severe category on a Saffir-Simpson scale. It killed 259 people on the Gulf Coast and further inland and caused an estimated 1.42×10^9 of damage (1969$).[2] Before it made landfall, it destroyed three Shell platforms and did much other damage to oil company infrastructure.

This paper revisits the properties of extreme waves measured well offshore in the Gulf of Mexico as the eye of Hurricane Camille passed close by in Aug. 1969 [1].

The analysis covers spectral analysis, wave asymmetry both vertical and horizontal, and the average shape of large waves via the NewWave formulation. Hence, it represents an extension of previous work on wave shape in nontropical winter storms [2,3]. Wave heights in Camille were measured using a Baylor wave staff, recorded on magnetic tape, and subsequently digitized at 0.1-s sampling rate [1]. The total duration spans 6 h from 1000 h to 1600 h local time. The records are divided into half-hour blocks.

As the motion of a hurricane causes a local storm surge, the effective mean-sea-level varies slowly as the hurricane passes.

For Hurricane Camille, the mean-sea-level rose about 0.15 m at the wave measurement point in 100 m of water (of course, closer inshore, this was dramatically amplified to a remarkable peak of 7.3 m). Thus, the Baylor wave staff data was first de-trended before further analysis was performed. Preliminary wave data analysis indicated that the 30-min recording from 15.15 to 15.45 had the most severe sea-state, with the highest significant wave height (H_s) of 13.3 m and the largest single wave (reported at the time as having a total height of 70 ft $\sim$ 21 m). Hence, the analysis concentrates on this period.

One of the important design criteria for offshore platforms is whether the wave hits the deck of the platform. If it does, the total force rises dramatically as a more solid deck structure is exposed to the waves. Thus, to prevent an occurrence of wave-in-deck loading, the nonlinearity of extreme waves has to be taken into account. The first order term in any wave field is responsible for the energy transport and is generally assumed to be consistent with linear random Gaussian statistics. The second order term affects crest and trough size—the sum double frequency (+) term simply makes crests taller and the difference (–) term produces long wave effects, setup, or set-down of the whole wave group.

In this article, we consider various aspects of the average shape of the largest crests and troughs in time, comparing Camille waves with NewWave, accounting for nonlinear bound wave components using a Stokes-type representation.

2 Average Shape of Large Waves

The shape of every individual wave on the open sea is unique. However, it is useful to examine the average shape associated with the large waves, as the wave kinematics are closely related to the wave shape. The 15:15–15:45 wave record contains about 170

---

[1]Corresponding author.
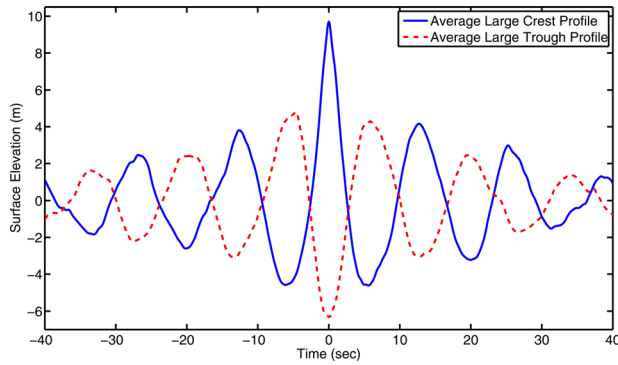[2]http://en.wikipedia.org/wiki/Hurricane_Camille.

Fig. 1 Average largest crest and trough profiles
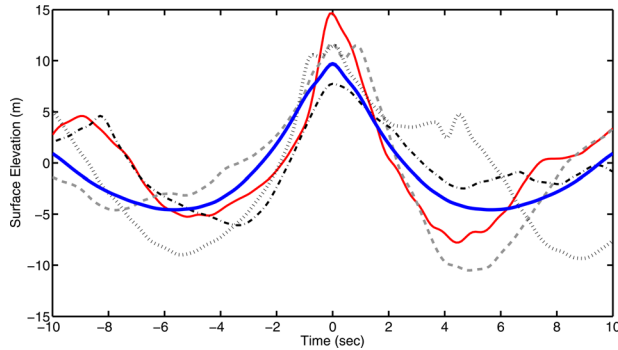
Fig. 2 Examples of the three largest crest time histories, the 20th largest, and the average of the largest 20

Fig. 3 Examples of the three largest trough time histories, the 20th largest, and the average of the largest 20

Fig. 4 Wave horizontal asymmetry comparison

waves. One way to construct an average representation of the largest crests and troughs in the real sea-state is by taking the average of the largest N crests and troughs, where we take N = 20 in this study. This step involves extracting the local time series of every crest and trough. The time series for each of the large crests is then shifted so the peak crest elevation occurs at zero (relative) time. Averaging is then performed across all of the crests lined up in time across a specified time interval, typically several wave periods. Here, we take the top 20 waves in the 30-min record with a time scale from –40 to 40 s centered at the conditioning event. The process is repeated with troughs to produce the average of the largest troughs. The two averaged profiles are shown in Fig. 1.

Both profiles appear close to symmetric in time (horizontal symmetry). There is a difference vertically: the crests are taller and narrower, while the troughs smaller and more rounded. These features are consistent, at least qualitatively, with second order theory.

To put these average wave profiles into context, Fig. 2 shows the time histories of the 3 largest crests, including the famous 70-ft high wave (with the crest at almost 15 m), the smallest one included in our average (the 20th largest crest), and the average of the 20 largest crests (shown in bold). Figure 3 shows the equivalent for troughs.

Clearly, analyzing the shape of the largest waves in a sea-state with a relatively short duration is challenging. For any individual large crest, there is considerable variation in both height and also shape in time. While it would be relatively simple to investigate this by random simulation in either a linear or second-order model (see, for example, Refs. [4] and [5]), instead, we estimate the variability in shape of large linear crests in a random sea-state using the rigorous statistical theory of Lindgren in Sec. 6 of this paper.

3 Wave Horizontal Symmetry

As well as the obvious vertical asymmetry between crests and troughs of waves in Hurricane Camille, the horizontal symmetry
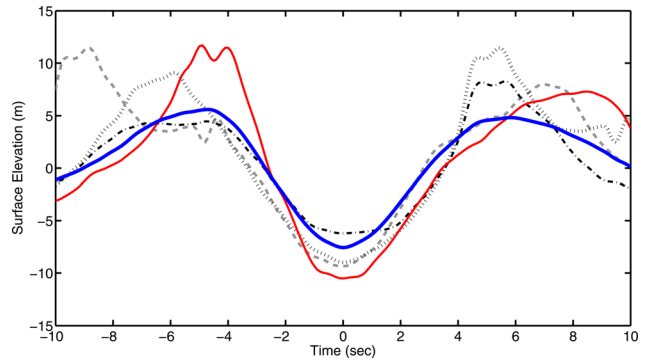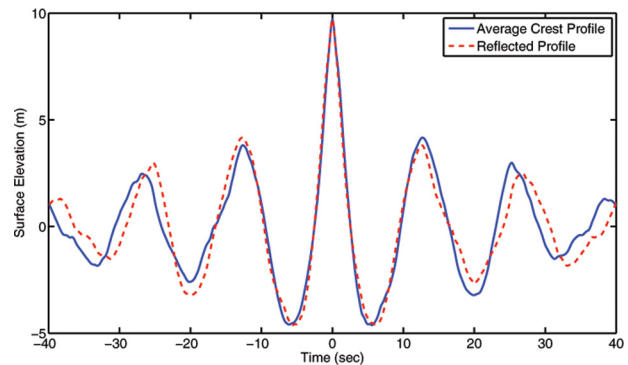
property of the waves is also examined. The idea is to justify horizontally symmetric models for the average shape of a large event, the shape of the local nonlinear bound wave corrections, and variance of individual waves around the average shape.

Clearly, wave breaking is an asymmetric process, obvious on a vertical spatial section as a plunging jet or spilling front on the forward face of the wave. How this physical process might be represented in a time history of surface elevation at a fixed point is perhaps less clear. However, it is likely that any net horizontal asymmetry on the upslope of a wave record in time is connected to wave breaking [6]. If the wave profiles are symmetric in time, it is not possible to tell which direction time runs in the wave record.

We first search for such asymmetry by plotting the average of the 20 largest crests in time and superimposing onto this plot its mirror image about the origin (t = 0), as shown in Fig. 4.

There is no obvious sign of asymmetry in time about the origin. There is perhaps an indication of a slight difference in shape between the troughs on either side of the central peak. Similar observations hold for the averaged trough shape. However, these are well within the range of statistical variation of the observations.

Another method is to measure wave heights of the entire 6-h record based on a zero up-crossing definition (trough to next crest in time) and then repeat this with a zero down-crossing definition (crest to next trough in time). The wave heights based on these two approaches are then sorted in ascending order and plotted against each other, whereby one axis is wave heights defined by crest then trough and the other axis is wave heights defined by trough then crest. Figure 5 plots the wave height comparison with zero up-crossing and down-crossing definitions. It is clear that the solid line matches the 1:1 line, except for the largest wave heights, where there is strong statistical variability. There is only slight evidence that the wave profile is weakly horizontally asymmetric for the largest waves, as the discrepancy away from the 1:1 line at
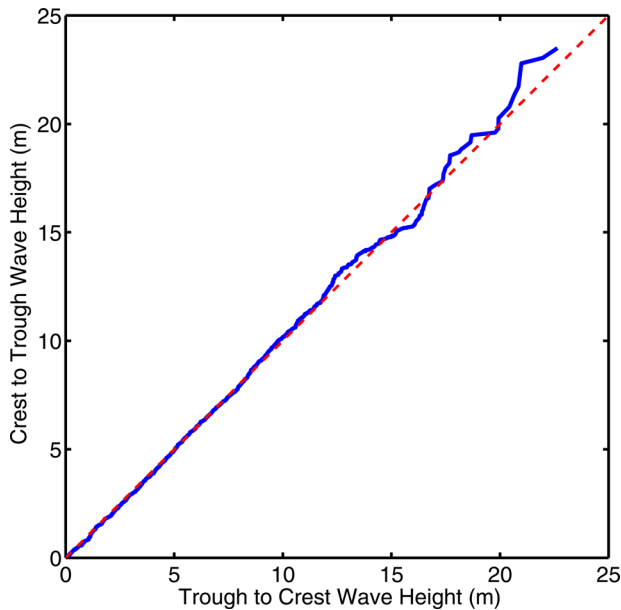
Fig. 5   C-T to T-C wave height comparison

the top end is only ∼ one standard deviation (based on estimates using bootstrapping [7]).

Our last method is related to the statistics of the maximum and minimum wave slopes. Numerical differentiation is an unstable process, so a better method, using Hilbert transforms, is applied [3]. The Hilbert transform introduces a 90 deg phase shift into the phase of the Fourier representation of the surface elevation data. Points of maximum gradient in the original record become points of maximum displacement away from the origin and vice versa. Thus, the crests of the Hilbert transformed surface elevation time-history are related to the steepest up-slopes in time of original waves, and the troughs of the Hilbert form are related to the down slopes.

The crests and troughs of the Hilbert transformed record are then sorted in ascending order and plotted against each other, as shown in Fig. 6. The data follows the dashed 1:1 line closely, except for the largest crests and troughs, where large sample variability again prevents any definitive conclusions from being drawn. As for the
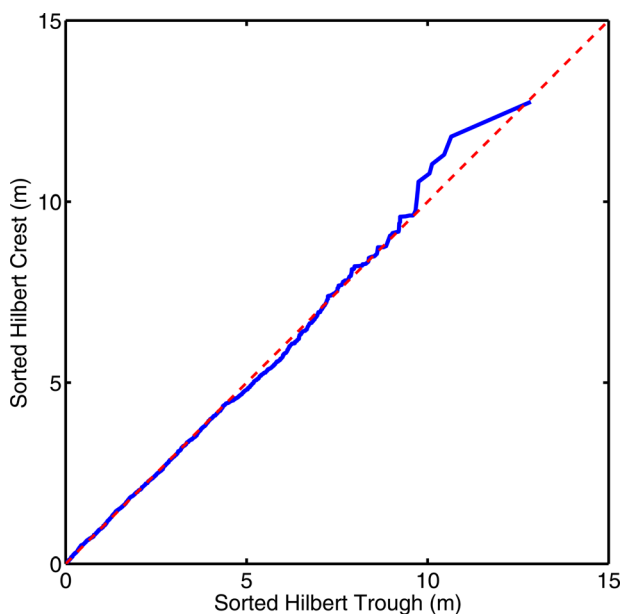

Fig. 6   Sorted Hilbert crests and troughs comparison

wave heights C-T and T-C, again, there is a small apparently systematic divergence for the largest Hilbert crests and troughs away from the 1:1 line. At the top end, this is again of the order of one standard deviation of the effective variability induced by finite sample size.

In short, there is only rather weak evidence of horizontal asymmetry, supporting the use of time-symmetric models to describe the structure of waves in Hurricane Camille.

We note that this work concentrates on the average shape of the largest waves within the Camille hurricane. Of course, there are some engineering problems, for which other wave parameters, such as wave slope, would be a more important parameter than peak crest elevation or wave height. For example, incoming wave slope is key for local wave impact pressures exerted on a vertical wall. Investigating wave parameters other than average wave shape would require analysis methods rather different from those used in this paper.

Although we stress the weak evidence of any meaningful asymmetry in the time records, it should be pointed out that both the C-T versus T-C and the Hilbert crest versus trough results match the rather obvious asymmetry in the largest (70 ft) wave in Camille—the trough ahead of the crest is smaller than the following trough *and* the maximum upslope on the crest is steeper than the maximum downslope. Further investigation is warranted.

4 Long Bound Waves

The second order difference or long wave contribution occurs at the difference frequencies of pairs of components of the main energy transporting linear elements of the wave field. In all seven storm conditions, these long bound waves produce local wave setup and set-down effects, which either add to or reduce the elevation of the peak crests. The size of the long waves scales with the local energy density of the wave field, but the sign as well as the size is affected by wave directional spreading. In close to unidirectional sea-states, typically of extra-tropical winter storms, long waves beneath the most energetic part of the waves tend to produce a set-down. In contrast, in crossing seas, linear wave components at more than ∼90 deg difference in incident angles to each other produce a setup instead. Walker et al. [8] give an example of such a setup for the Draupner New Year wave. There, a peak elevation of 18.5 m was recorded in a sea-state with a significant wave height of approximately 12 m, and the paper demonstrated a quite prominent setup of about 0.5 m beneath the giant crest.

Here, the long bound wave is obtained by low pass filtering the frequency spectrum of the 15:15–15:45 record at low pass upper cut off frequency of $0.5\omega_p$ to minimize the linear contribution passed through the filter and maximize the second-order difference contribution, where ω_p is the frequency corresponding to the peak of the spectrum.

We present the averaged long wave component in time conditioned on the largest crest and troughs occurring at zero relative time (t = 0). Rather than the 20 events taken previously, the long wave averaged time histories are based on 18 large crests and 19 large troughs. The other 2 large crests and 1 large trough could not be included, as they occur too close to the ends of the record to permit accurate low pass filtering. These long waves are then combined to obtain the averages, shown in Fig. 7. The long waves for large crests and troughs are similar, each having a very small central setup of ∼5 cm associated with linear wave components with amplitudes of ∼8 m.

We cannot apply second order wave theory to predict this setup, as there are no directional spreading estimates available to us for waves in Hurricane Camille. However, the tiny magnitude is consistent with the work of Dalzell, who showed that, for deepwater waves, the long wave effect should be very small [9]. The sign of the long wave as a setup term is consistent with a rather directionally spread sea-state (see Adcock and Taylor [10]).

In a hurricane where the rapidly rotating and moving strong wind field creates wave components moving in many directions,
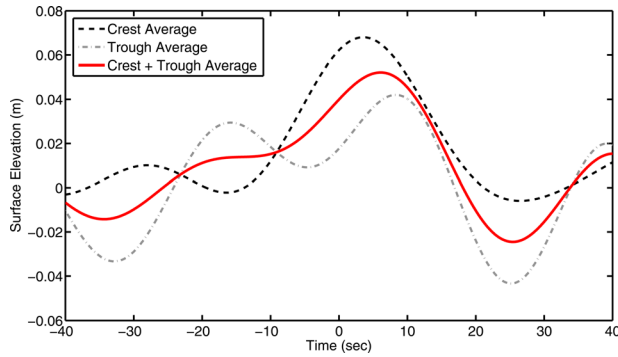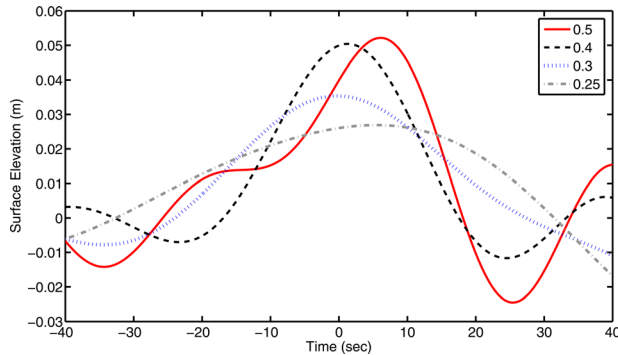
Fig. 7 Average long bound wave profile

Fig. 8 Average long bound wave with different upper cutoff frequencies (ω/ω_p as shown)

we might expect that the long bound waves do not show any significant set-down effects below energetic wave groups, and here we see only a tiny setup of no practical significance for determining maximum crest height.

To check the robustness of the long wave results, different upper cut off frequencies were applied, and the resultant long bound waves are plotted in Fig. 8. The small setup appears to be a robust result.

5 Average Wave Shapes and Nonlinear Sum Harmonics

A Stoke expansion represents a complete regular wave as a sum of components of increasing order from linear, second order, third order, and so on. In this paper, we aim to fit the shapes of the average of the top 20 crests and troughs using a linear model with approximations for the sum harmonics. Following Walker et al. [8], we write the Stokes expansion for a regular wave to third order as

$$\eta(t) = a\cos(\omega t) + \frac{S_{22}}{d}a^2\cos(2\omega t)$$
$$+ \frac{S_{33}}{d^2}a^3\cos(3\omega t) + \dots \tag{1}$$

This has the advantage over the conventional form that the coefficients S_{22}, etc. are solely functions of the nondimensional water depth kd. Assuming the slowly varying (narrow banded) linear component is $\eta_L(t) \approx a\cos(\omega t)$, its Hilbert transform simply requires a phase shift of 90 deg to give $\eta_{LH}(t) \approx a\sin(\omega t)$. We can then use the standard multiple angle formula to approximate the second and higher order sum harmonics as

$$\eta_L^2 - \eta_{LH}^2 \approx a^2\cos(2\omega t) \tag{2}$$

Lindgren [11] and Boccotti [12] showed that the average shape of a large extreme in a linear random Gaussian process tends to the

autocorrelation function. In much previous work, we have described this result as NewWave [2,3,8]. With a long wave record, it is simple to compute the autocorrelation function as the Fourier transform of the energy spectrum. Here, we bandpass the spectrum over the interval $0.5\omega_p$ to $10\omega_p$. Very low frequency components are small, but are discarded to eliminate the contribution from second-order difference (long bound waves). The high frequency components are limited to $10\omega_p$, as analysis of the spectral tail suggests that, above this frequency, the data may not be physically meaningful.

We now seek to model the average shape of the large crests and troughs shown in Fig. 1 in terms of the NewWave profile and its harmonics as shown above. The target functions are fitted using a kernel estimation method, the kernel being the square root of the envelope of NewWave in time. This is used rather than a uniform weighting over the whole 80-s duration of the signals in Fig. 1, because we are much more confident of the structure of the wave close to the center of the interval, where the sampled large waves were all aligned prior to averaging across all the samples.

We take the linear component as a NewWave of unit amplitude, scaled to a linear magnitude of A, so

$$\eta_L = \rho(t) = \frac{1}{\sigma^2}\int_0^\infty S(\omega)\cos(\omega t)dx \tag{3}$$

The bound harmonics are approximated in terms of NewWave and its Hilbert transform, as explained earlier. Hence, the fit determines the best representation of the shapes of the average of the top 20 crests and troughs in terms of the function

$$\eta(t) = A\eta_L + \frac{S_{22}}{d}A^2(\eta_L^2 - \eta_{LH}^2)$$
$$+ \frac{S_{33}}{d^2}A^3(\eta_L^3 - 3\eta_L\eta_{LH}^2) + \dots \tag{4}$$

giving as output the linear amplitude A at the time origin ($t = 0$) and the Stokes-like coefficients S_{22} and S_{33}, given in Table 1. The water depth is assumed to be 100 m [1].

The fits to the averaged crest and trough shapes are shown in Figs. 9 and 10. All the main features are well represented: higher and narrower crests and flatter and shallower troughs. Although the net contribution of the third order sum term is small in amplitude, it does slightly improve the fit at the central peak for the averaged crest. Although small in amplitude, it significantly increases the curvature and forces the crest above mean-sea-level to be narrower. Also shown on the figures is a fit using the averaged numerical values of the coefficients S_{22} and S_{33}. These fits are less good for the crest, with an undershoot at the peak of the crest.

We obtain the following results:

The values for the Stokes coefficients are for a regular wave period of 12 s. One interesting feature is the difference in the linear
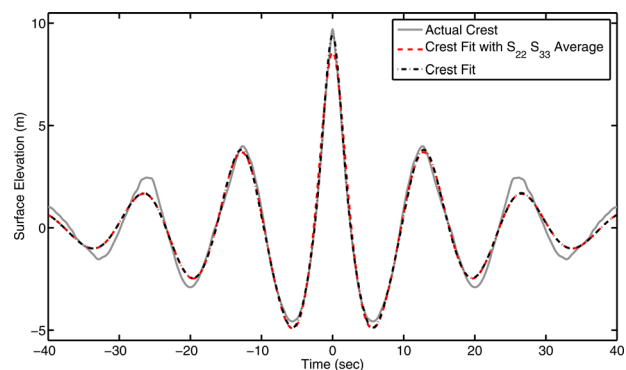

Fig. 9 Average measured crest, individual harmonic fit, and a fit using averaged coefficients
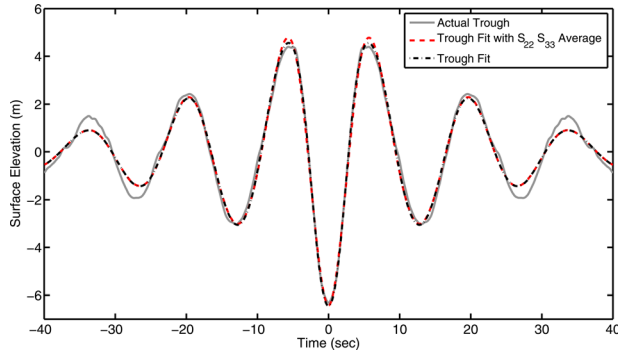
Fig. 10   Average measured trough, individual harmonic fit, and a fit using averaged coefficients

Fig. 11   Comparison of the measured versus Lindgren variance profile

amplitudes; this presumably arises by chance, but explains why we are forced to fit the whole harmonic structure in one go rather than adding and subtracting the averaged crest and trough time histories to give even and odd components separately, as in previous work [2,3,8]. We see that the average of the fit-based estimates of the second order coefficient S_{22} is slightly smaller than regular wave Stokes theory would predict. Previous work suggests that this reduction may be due to directional spreading [2,10]. The third order coefficient is much more variable, actually negative for the averaged trough. We have no simple explanation for this other than the size of the expected third order harmonic compared to the statistical variation for a fit based on only 20 waves. However, since the Baylor wave gauge has to be fixed onto the structure, the measurements may suffer from some interference due to waves hitting structural members. This can only be a weak effect, as the linear NewWave type behavior appears satisfactory, as does horizontal symmetry of the records. However, a small degree of interference could be enough to impair our estimates of the coefficients S_{22} and, particularly, S_{33}.

Overall, we confirm that NewWave, previously tested for winter storm data for waves measured on both deep water in the northern North Sea conditions and also on shallow water in the southern North Sea, also fits well to the average of the largest waves generated by Hurricane Camille, a tropical storm.

We also find that the shape of the dominant second order nonlinear contribution can be modeled using a harmonic approximation based on NewWave.

6   Variability and Standard Deviation of the Largest Wave Profiles

The comparison of the averaged largest crest and trough profiles in Sec. 5 to the fits based on the NewWave autocorrelation function with the bound harmonics seems to work well. However, there is a need to justify statistically the fit of the two curves. The standard procedure involves determination of the variance and standard deviation of each of the individual large crests to the average large crest and this mean of the samples to the true mean.

The variance between the individual time histories and the average is defined in the usual way,

$$\text{Variance}(t) = \frac{1}{N} \sum_{i=1}^{N} [\eta_i(t) - \bar{\eta}(t)]^2 \qquad (5)$$

where $\eta_i(t)$ is the i-th individual large crest profile, $\bar{\eta}(t)$ is the average large crest profile, and $N = 20$ is the number of individual large crests included.

Theoretically, at zero time, where the largest crest (or trough) occurs, the variance and the standard deviation of the samples around the peak is zero—if the waves selected all have exactly the same crest value. However, as the twenty largest crests and troughs extracted have considerable variation in terms of the peak
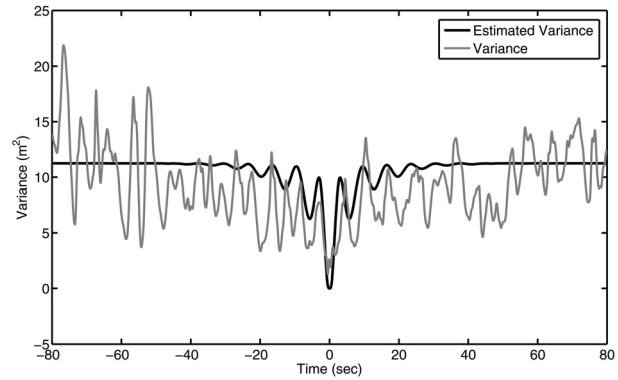
crest height and trough depth (as shown in Fig. 2), so the variance cannot reduce to zero there. Of course, when processing field data from the random natural environment, one cannot possibly control the magnitude of the largest crests and troughs.

For a linear random Gaussian process, Lindgren [11] derived an asymptotic expression for the variation in shape of individual crests around the expected shape of the scaled autocorrelation function (NewWave). This is given in Taylor et al. [13] as

$$\text{Lindgren Variance}(t) = \sigma^2 \left(1 - \eta_L^2 - \frac{\eta_{Lt}^2}{\lambda^2} \right) \qquad (6)$$

where $\eta_L = 1/\sigma^2 \int S(\omega) \cos(\omega t) d\omega$, as before, and $\eta_{Lt} = 1/\sigma^2 \int \omega^2 S(\omega) \sin(\omega t) d\omega$ with $\lambda^2 = 1/\sigma^2 \int \omega^2 S(\omega) d\omega$.

Here, η_L is the NewWave autocorrelation function and η_{Lt} is related to the autocorrelation function for vertical velocity of the wave; λ^2 is proportional to the variance of the free-surface vertical velocity.

Figure 11 shows the plot of the theoretical Lindgren variance with the actual measured variance. The agreement between the two curves is considered adequate, with so few samples ($N = 20$) given that variance is error squared. Quite rapidly, this constrained variance tends to a value of $\sigma^2 = H_S^2/16 = 11.1 \text{m}^2$, that of the underlying random process.

Again discussed earlier, the measured variance local to the constraint time of ($t = 0$) does not drop to zero. However, it does reduce to $O(\sim 10\%)$ of the background, which we deem to be acceptable.

A second reason for estimating the Lindgren variance is that we can use it to estimate a tolerable level of mismatch between the theoretical models in Sec. 5 and the average of the top 20 crests. In Fig. 12, we re-plot Figs. 1 and 9 for the crests, now with bands of ± 2 standard deviations of the estimated position of the mean profile
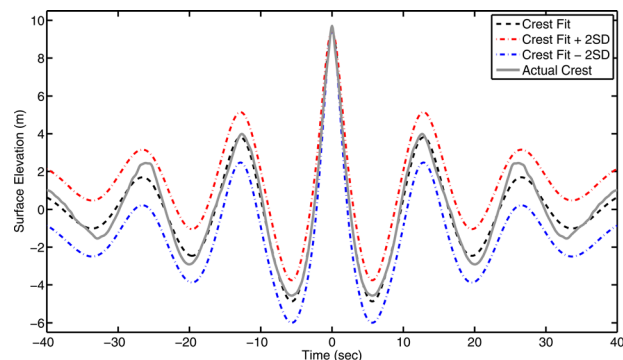

Fig. 12   Time history of the mean of largest crests with bands of ±2 standard deviations of the estimate of the mean, based on Lindgren's model

(the Lindgren standard deviation/$\sqrt{20}$). It is clear that the nonlinear model fits the measured average crest to well within ± 2 times the theoretical standard deviation. So we conclude that NewWave with nonlinear harmonics is a reasonable model for hurricane waves.

Clearly, this comparison could be repeated for the top 5 or 10 waves in the record, which are of more interest simply because they are larger. Unfortunately, the standard deviation for 5 compared to 20 waves will be twice as large, showing the large variability associated with the largest waves in a sea-state both in magnitude, but also in shape.

7 Spectral Tail Analysis

The final piece of analysis of wave data for Camille concerns the high frequency power law decay of the spectral tail. The power spectrum of the 15:15–15:45 record is shown in Fig. 13. The spectral peak corresponds to a wave period $T_p \sim 13.7$ s, and the spectrum shown is based on the average of 15 successive points from the FFT.

The spectrum is replotted on log scales in Fig. 14, which also shows lines corresponding to ω^{-4} and ω^{-5} to help judge what value of power law is most appropriate.

It is difficult to decide exactly which slope to choose; the power is clearly between –4 and –5. Despite Fig. 14 appearing to show that the slope is closer to –5, we estimate that there is approximately one decade in frequency with a decay rate of $\omega^{-4.5}$, as determined by plotting $(\omega, \omega^{4.5}S(\omega))$ on log scales (not shown), but, beyond $\omega \sim 4$ rad/s (a wave period of 1.6 s), the spectral tail slope changes and appears noisier. The standard Pierson–Moskowitz and JONSWAP model spectra have ω^{-5} tails. Our
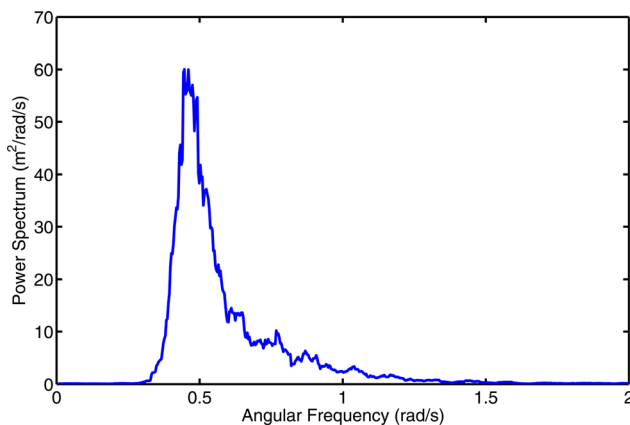
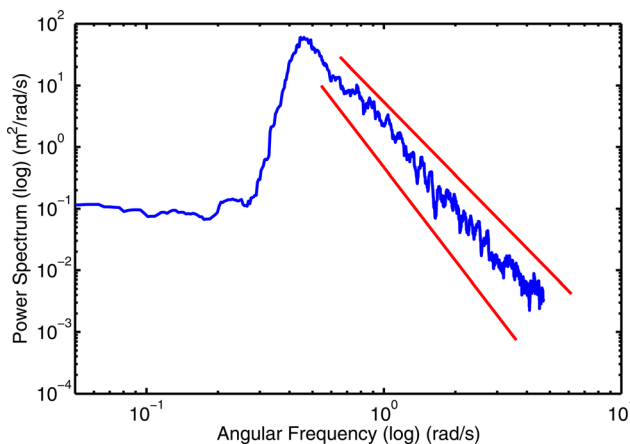

Fig. 13 Wave spectrum from Camille

Fig. 14 Wave spectrum in log scale

Table 1 Comparison between values obtained with the Stokes theory

	A (m)	S_{22}	S_{33}
Crest	+7.80	+1.73	+11.8
Trough	−6.85	−0.38	−11.0
Mean		1.05	0.4
Stokes		1.45	3.1

result is midway between the original form and the slightly flatter ω^{-4} tail proposed by Battjes et al. [14], who reanalyzed the original JONSWAP data.

8 Conclusion

The current study has been undertaken to look at various features of steep waves in tropical storms. We find that the average shapes of the 20 highest crests and deepest troughs in the most severe 30 min segment of wave data from Hurricane Camille are very close to symmetric in time, with only very slight evidence for wave breaking on the averaged profile. Of course, significant wave breaking is to be expected in such a severe sea-state. We simply cannot resolve this well in our averaged approach. We note, though, the slight indications of weak asymmetry in time that we identify are both consistent with the obvious asymmetry of the famous 70-ft wave in Hurricane Camille.

The waves show considerable vertical asymmetry with clearly higher and sharper crests and smaller and more rounded troughs. There is a robust but small setup below both the largest crests and troughs of height ~ 50 mm, suggesting that the hurricane wave fields are highly directionally spread.

The shapes of the averaged profiles can be fitted well with a large linear NewWave and the second and third sum harmonics based on a Stokes-like expansion in terms for products of the autocorrelation (NewWave) and its Hilbert transform. However, the estimated magnitudes of the two fitting coefficients show considerable variation between crests and troughs, which may be related to the small number of events that can be included in the fitting. The average value of the second order sum coefficient is found to be relatively close to but smaller than the value from Stokes regular wave theory, again consistent with a highly directional spread wave field.

Finally, the power law decay of the high tail of the wave energy spectrum is analyzed. A $\omega^{-4.5}$ power is established between the classical JONSWAP –5 form and the –4 proposed by Battjes et al.

Acknowledgment

References

[1] Earle, M. D., 1975, "Extreme Wave Conditions During Hurricane Camille," J. Geophys. Res., **80**(3), pp. 377–379.

[2] Jonathan, P., and Taylor, P. H., 1997, "On Irregular, Nonlinear Waves in a Spread Sea," ASME J. Offshore Mech. Arct. Eng., **119**, pp. 37–41.

[3] Taylor, P. H., and Williams, B. A., 2004, "Wave Statistics for Intermediate Depth Water—NewWaves and Symmetry," ASME J. Offshore Mech. Arct. Eng., **126**, pp. 54–59.

[4] Forristall, G. Z., 2000, "Wave Crest Distributions: Observations and Second-Order Theory," J. Phys. Oceanogr., **30**(8), pp. 1931–1943.

[5] Prevosto, M., and Forristall, G. Z., 2004, "Statistics of Wave Crests From Models vs. Measurements," ASME J. Offshore Mech. Arct. Eng., **126**, pp. 43–50.

[6] Ochi, M. K., 1998, Ocean Waves: The Stochastic Approach, Cambridge University, Cambridge, England.

[7] Diaconis, P., and Efron, B., 1983, "Computer-Intensive Methods in Statistics," Sci. Am., **248**(5), pp. 116–129.

[8] Walker, D. A. G., Taylor, P. H., and Eatock Taylor, R., 2005, "The Shape of Large Surface Waves on the Open Sea and the Draupner New Year Wave," Appl. Ocean. Res., **26**(3–4), pp. 73–83.

[9] Dalzell, J. F., 1999, "A Note on Finite Depth Second-Order Wave-Wave Interactions," Appl. Ocean. Res., **21**(3), pp. 105–111.

[10] Adcock, T. A. A., and Taylor, P. H., 2009, "Estimating Ocean Wave Directional Spreading From an Eulerian Surface Elevation Time History," Proc. R. Soc. London, Ser. A, **465**(2111), pp. 3361–3381.

[11] Lindgren, G., 1970, "Some Properties of a Normal Process Near a Local Maximum," Ann. Math. Stat., **41**(6), pp. 1870–1883.

[12] Boccotti, P., 1983, "Some New Results on Statistical Properties of Wind Waves," Appl. Ocean. Res., **5**(3), pp. 134–140.

[13] Taylor, P. H., Jonathan, P., and Harland, L. A., 1997, "Time Domain Simulation of Jack-Up Dynamics With the Extremes of a Gaussian Process," ASME J. Vib. Acoust., **119**, pp. 624–628.

[14] Battjes, J. A., Zitman, T. J., and Holthuijsen, L. H., 1987, "A Reanalysis of the Spectra Observed in JONSWAP," J. Phys. Oceanogr., **17**(8), pp. 1288–1295.